

Magnetic Moments and Unpaired Spin Densities in the Fe-Rh Alloys*

G. SHIRANE AND R. NATHANS

Brookhaven National Laboratory, Upton, New York

AND

C. W. CHEN

Westinghouse Research Laboratories, Pittsburgh, Pennsylvania

(Received 22 January 1964)

The distribution of magnetic moments in the Fe-Rh system has been investigated by the neutron diffraction technique in the composition range between 35 and 50 at. %Rh. These alloys have chemical order of CsCl type; the body-corner positions are occupied by FeI atoms and the body centers by Rh and FeII atoms. The magnetic moments in ferromagnetic alloys containing 35, 40, and 48% Rh are $\mu_{\text{FeI}} = 3.1 \mu_B$, $\mu_{\text{FeII}} = 2.5 \mu_B$, and $\mu_{\text{Rh}} = 1.0 \mu_B$ at 25°C. The moment of the FeI atom in the 50% Rh alloy, which is antiferromagnetic at room temperature, increases to $3.3 \mu_B$. A detailed study of the unpaired spin density distribution in the 48% Rh alloy was made by the polarized beam technique. While the FeI atom has a nearly spherical density distribution, that of the Rh atom shows a strong tendency towards e_g symmetry. The coherent nuclear scattering amplitude of Rh was determined to be $0.585 \pm 0.005 \times 10^{-12}$ cm.

I. INTRODUCTION

IN a previous paper¹ we have reported a systematic investigation of the Fe-Rh alloys by the Mössbauer technique. Up to 52% Rh these alloys possess a body-centered cubic lattice in which there is chemical order of CsCl type when the Rh concentration exceeds 20%. In the ordered alloys, iron atoms located at the body corners are labeled FeI and those in the Rh sites at the body centers FeII (see the insert to Fig. 1). The system exhibits two interesting magnetic properties. First, fairly large moments are observed over a wide concentration range,^{1,2} as shown in Fig. 1. Second, a ferromagnetic-antiferromagnetic transition^{3,4} occurs in alloys containing around 50% Rh. The transition temperature increases with increasing Rh concentration, and is observed to be 65°C in the 50% Rh alloy. The room temperature phase changes from ferromagnetic to antiferromagnetic between 49% and 50% Rh.

The Mössbauer measurements¹ revealed two distinct hyperfine fields in ordered alloys, corresponding to FeI and FeII. For example, $H_i(\text{I})$ and $H_i(\text{II})$ were found to be 277 and 384 kOe, respectively, in an alloy containing 48% Rh. It was suggested that FeII, which is surrounded by 8 Fe nearest neighbors, may have a smaller magnetic moment than FeI despite its higher hyperfine field. The main interest in this alloy system therefore lies in the composition dependence of both the moments and the hyperfine fields of FeI, FeII, and Rh.

A neutron diffraction study of the FeRh alloy was

first carried out by Bertaut, de Bergevin, and Rault.⁵ Using powder data, they reported $\mu_{\text{Fe}} = 2.8 \mu_B$ and $\mu_{\text{Rh}} = 0.8 \mu_B$ for the 53% Rh alloy in the ferromagnetic region above 60°C. The present work describes neutron diffraction measurements of the magnetic moments of FeI, FeII, and Rh in ordered alloys, and a detailed study of the spin density distribution of Fe and Rh in the 48% Rh alloy. A study of the 50% Rh alloy, which is antiferromagnetic at room temperature, was also made.

II. EXPERIMENTAL

A. Samples

The alloys used in this work are those previously investigated by the Mössbauer technique. All alloys

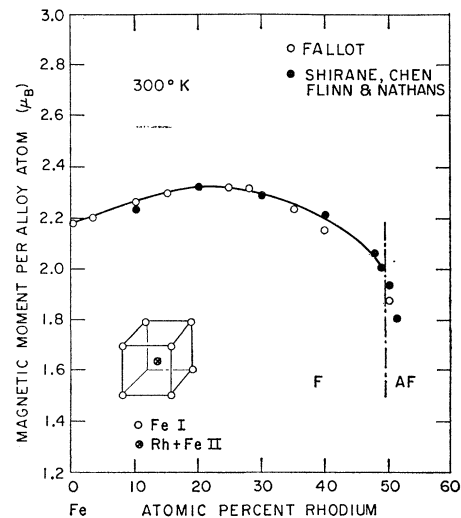


FIG. 1. Average atomic moments of Fe-Rh alloys at 300°K. The values in the antiferromagnetic phase were obtained by extrapolation of the data obtained for the high-temperature phase.

* Work supported by the auspices of the U. S. Atomic Energy Commission and the Advance Research Project Agency.

¹ G. Shirane, C. W. Chen, P. A. Flinn, and R. Nathans, *Phys. Rev.* **131**, 183 (1963).

² M. FalLOT, *Ann. Phys. (Paris)* **10**, 291 (1938); M. FalLOT and R. Hocart, *Rev. Sci.* **77**, 498 (1939).

³ F. de Bergevin and L. Muldower, *Compt. Rend.* **252**, 1347 (1961).

⁴ J. S. Kouvel and C. C. Hartelius, *J. Appl. Phys. Suppl.* **33**, 1343 (1962).

⁵ F. Bertaut, F. de Bergevin, and G. Rault, *Compt. Rend.* **256**, 1668 (1963).

TABLE I. Physical properties of Fe-Rh alloys. The moment value of 50% Rh (*) is obtained by extrapolation from the ferromagnetic phase above 65°C.

Composition	48% Rh	50% Rh
Lattice constant	2.989 Å	2.986 Å
Curie temperature	500°C	405°C
Magnetic moment per atom, 300°K	2.07 μ_B	1.94 μ_B^*
Néel temperature	...	65°C

were prepared from high-purity metals by levitation melting with subsequent heat treatments as described in the previous paper.¹ The chemical analysis agreed with the nominal composition within 0.5 at.%. Single crystals large enough for neutron diffraction study were obtained by levitation melting of the 48 and 50% Rh alloys. Efforts to grow single crystals of the 25% Rh alloy by the electron beam technique were not successful. This may be due to the existence of a γ phase at high temperatures. An attempt to obtain single crystals of the 35% Rh alloy by the stress annealing technique was also unsuccessful.

Thus polycrystalline samples containing 35 and 40% Rh were used to study the moments of FeI and FeII. Detailed studies of the ferromagnetic and antiferromagnetic phases were carried out on the 48% Rh and 50% Rh single crystals, respectively. The magnetic properties of these two alloys are listed in Table I.

Interpretation of the magnetic diffraction data

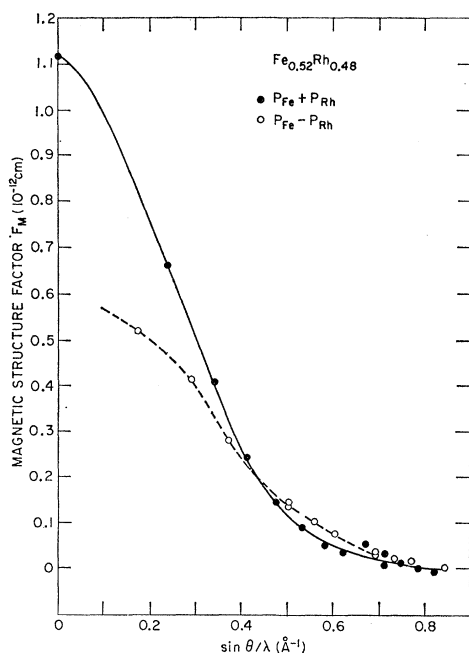


FIG. 2. The observed magnetic structure factors F_M , of $\text{Fe}_{0.52}\text{Rh}_{0.48}$. Reflections with $h+k+l=2n$ are shown by solid circles, those with $h+k+l=2n+1$ by open circles. The point at $\sin\theta/\lambda=0$ corresponds to the observed bulk moment of 4.14 μ_B .

requires a precise knowledge of the chemical order in these alloys. Previous Mössbauer measurements, coupled with x-ray powder patterns, had revealed pronounced order in all the alloys containing more than 20% Rh. A careful study of the 50% Rh alloy, to be described later, showed that ordering is complete. Somewhat less accurate measurements on the 35% and 48% alloys gave a similar result.

B. Polarized Neutron Technique

Except for the study of the antiferromagnetic phase containing 50% Rh, all the measurements were made with the use of the polarized neutron technique, which has already been described in detail.⁶⁻⁹ By reversing the incident neutron polarization, we measure the polarization ratio

$$I_{(+)} / I_{(-)} = (1 + \gamma)^2 / (1 - \gamma)^2,$$

where γ is the ratio of the magnetic to the nuclear structure factor (F_M/F_N). The observed ratios were corrected for incomplete polarization of the incident beam (0.98) and for incomplete polarization reversal (0.98).

It is also necessary to make allowance for multiple scattering processes within the crystal. It has been shown⁹ that multiple scattering can introduce serious errors in the measured polarization ratios. In order to detect and eliminate this effect, the crystals were mounted on a goniometer in a magnetizing field of 10 kOe, and the polarization ratio was studied as a function of the azimuthal angle around the scattering vector.

III. SPIN DENSITY IN FERROMAGNETIC $\text{Fe}_{0.52}\text{Rh}_{0.48}$

Single crystals were cut into the shape of pillars, roughly 2×3 mm in cross section and 15 mm in length, with their long axes along $[110]$ and $[100]$, respectively. In addition, a smaller cylindrical $[110]$ crystal (1-mm diam), which was cold worked, was used to check for possible extinction effects in strong reflections. Extinction effects were also investigated by mis-setting the Bragg angle.⁶ Even for undistorted crystals, extinction corrections were proved to be negligible except for the two strongest reflections.

Intensity measurements were made out to an angle corresponding to $\sin\theta/\lambda = 0.85 \text{ \AA}^{-1}$, with a wavelength of 1.05 Å. The number of reflections totaled 26, and all except two, (321) and (421), are contained in the two zones. The results are shown in Fig. 2 and Table II. In calculating the magnetic structure factor F_M from the relationship $\gamma = F_M/F_N$ we used $b_{\text{Fe}} = 0.951^9$ and $b_{\text{Rh}} = 0.585 \times 10^{-12} \text{ cm}$, the latter value being determined from the 50% Rh alloy (see Sec. V). The errors quoted

⁶ R. Nathans, C. G. Shull, G. Shirane, and A. Andresen, Phys. Chem. Solids **10**, 138 (1959).

⁷ R. Nathans, Suppl. J. Appl. Phys. **31**, 350 (1960).

⁸ S. J. Pickart and R. Nathans, Phys. Rev. **123**, 1163 (1961).

⁹ C. G. Shull and Y. Yamada, J. Phys. Soc. Japan **17**, Suppl. B III, 1 (1962).

in Table II are the standard deviations of repeated measurements.

In the CsCl type of structure, the structure factors F_M are divided into two kinds,

$$F_M = p_{\text{Fe}} + p_{\text{Rh}} \quad \text{for } h+k+l=2n,$$

$$F_M = p_{\text{Fe}} - p_{\text{Rh}} \quad \text{for } h+k+l=2n+1,$$

where p_{Fe} and p_{Rh} are the magnetic scattering amplitudes of Fe and Rh, respectively, and are equal to the product of the magnetic moment μ and the form factor f ,

$$p_{\text{Fe}} = \mu_{\text{Fe}} f_{\text{Fe}}, \quad p_{\text{Rh}} = \mu_{\text{Rh}} f_{\text{Rh}}.$$

Figure 2 clearly shows that these two groups of reflections lie on two separate curves which cross each other around $\sin\theta/\lambda = 0.45 \text{ \AA}^{-1}$. This implies that the rhodium form factor f_{Rh} becomes negative at this point, in agreement with recent calculations by Watson and Freeman.¹⁰ Thus it falls off much more rapidly as a

TABLE II. Magnetic structure factors F_M , in units of 10^{-12} cm, per CsCl type unit cell of $\text{Fe}_{0.52}\text{Rh}_{0.48}$.

hkl	$F_M(\pm 0.001)$	hkl	$F_M(\pm 0.002)$
100	0.516	011	0.658
111	0.410	200	0.400
120	0.275	211	0.237
{300	0.136	022	0.141
{122	0.144	130	0.090
311	0.104	222	0.053
230	0.076	321	0.035
{322	0.039	400	0.052
{140	0.037	{033	0.009
133	0.023	{411	0.030
421	0.016	240	0.012
{500	0.003	233	0.000
{430	0.004	422	-0.010

function of the scattering angle than the form factor of Fe, which becomes negative only above $\sin\theta/\lambda = 0.80 \text{ \AA}^{-1}$.

These data were analyzed in two ways. The first is the direct comparison of observed and calculated structure factors, and the second involves the Fourier inversion of the data. We shall describe the second approach first, since it gives a more visible picture. This process of Fourier inversion was used by Pickart and Nathans⁸ for Fe_3Al and Shull and Yamada⁹ for Fe. Our preliminary analysis was made with a Fourier projection on the (110) plane, but a heavy overlap due to an extended wave function of Rh made the three-dimensional Fourier analysis desirable.

Following conventional crystallographic notation, we have

$$\rho(xyz) = (1/V) \sum F_{hkl} \cos 2\pi(hx + ky + lz),$$

where ρ is the magnetic spin density and V is the unit cell volume. The summation has been carried out on

¹⁰ R. E. Watson and A. J. Freeman (unpublished).

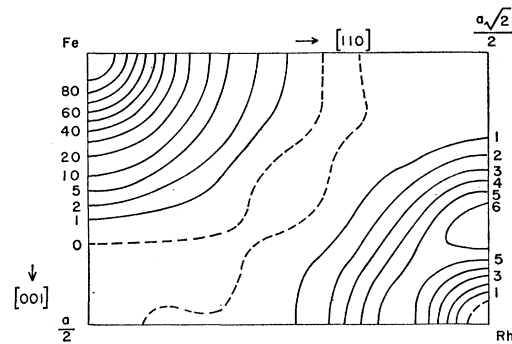


FIG. 3. Magnetic moment density distribution in the (110) plane. The scale is taken to give 100 at the Fe nucleus, which corresponds to $6.82 \mu_B/\text{\AA}^3$.

the computer. Figure 3 illustrates a portion of the (110) plane intersecting the two atoms in the unit cell. This Fourier map clearly illustrates the lobe along the [001] axis for Rh, the characteristic of e_g symmetry. On the other hand, the Fe density distribution corresponds more closely to spherical symmetry. Figure 4 illustrates the moment density along two principal directions, [001] and [111], the latter being directed towards the nearest neighbors. This figure shows that the Fe spin density also shows some deviation towards e_g symmetry, in that the density along [001] is slightly higher than that along [111] at the equivalent distance.

It is emphasized that the large difference in the angular dependence of the form factors, f_{Fe} and f_{Rh} , has a significant effect on their Fourier contours. Available data within the given angle of $\sin\theta/\lambda = 0.85 \text{ \AA}^{-1}$ allow an excellent resolution of the Rh spin density distribution to be made since its form factor crosses zero at

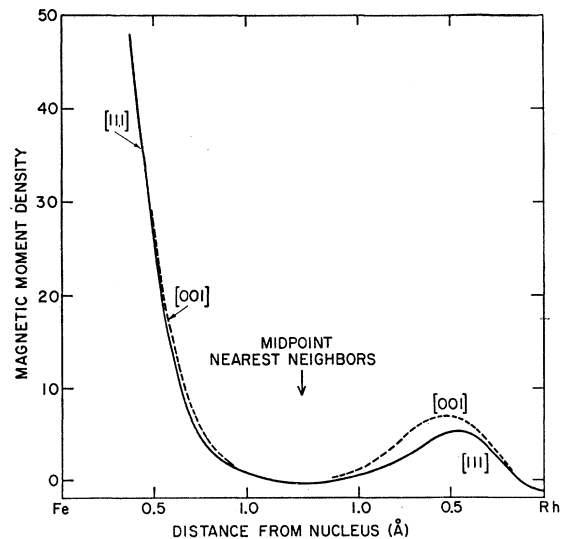


FIG. 4. Magnetic moment density distribution in the [001] and [111] directions as a function of distance from the nuclei. The scale 10 corresponds to $0.68 \mu_B/\text{\AA}^3$. [111] corresponds to the nearest-neighbor direction.

$\sin\theta/\lambda=0.45 \text{ \AA}^{-1}$. We may note that the magnetic moment density at the Rh nucleus is almost zero as would be expected if the magnetic moment arises from the presence of unpaired d electrons. On the other hand, the densities near the Fe nucleus are considerably distorted by the series termination error.

The magnetic moments of the Fe and Rh atoms were estimated in the following manner. Since the density distribution shown in Fig. 3 does not show any overlap, the integration of the densities around each of the atoms, namely $\sum \rho(r)4\pi r^2$, gives their magnetic moments. This method gives $\mu_{\text{Fe}}=3.17\pm 0.10 \mu_B$ and $\mu_{\text{Rh}}=0.97\pm 0.10 \mu_B$. These values are subject to errors which result from the fact that only a finite number of reflections are used in the construction of a Fourier map. The effect of this series termination error on magnetic density was studied in detail by Pickart.¹¹ From this study we can estimate that in the present case the error is not more than a few percent for Fe. Another estimate was made directly from the data shown in Fig. 2. We draw a smooth curve through the observed points, taking into account the asphericity. Then for a given observed value of $p_{\text{Fe}}+p_{\text{Rh}}$, that of $p_{\text{Fe}}-p_{\text{Rh}}$ can be estimated with reasonable accuracy. In this way we can obtain p_{Fe} and p_{Rh} uniquely as a function of $\sin\theta/\lambda$. Then $p_{\text{Fe}}=\mu_{\text{Fe}}f_{\text{Fe}}$ were compared with the form factor of Fe metal.

If we now assign a value of $3.14 \mu_B$ to the FeI moment, it may be seen from Fig. 5 that the form factor thus obtained is almost identical to that of Fe metal as

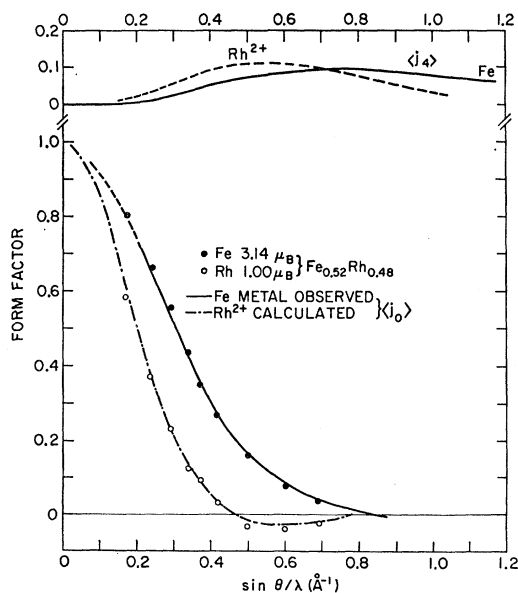


FIG. 5. Estimated form factors of Fe and Rh, as described in the text. The observed form factor of Fe metal (Ref. 9) is shown by the solid line and the calculated form factor (Ref. 10) of Rh^{2+} by the broken line. The calculated aspherical terms $\langle j_4 \rangle$ are shown at the top.

¹¹ S. J. Pickart, Acta Cryst. 16, 174 (1963).

determined by Shull and Yamada⁹ over a quite wide angular range. This Fe moment, combined with the observed bulk moment of $4.14 \mu_B$, gives $\mu_{\text{Fe}}=3.14 \mu_B$, $\mu_{\text{Rh}}=1.0 \mu_B$.

At present, theoretical form factors¹⁰ for Rh are available only for Rh^{2+} and Rh^{3+} . The observed form factor f_{Rh} turns out to be in excellent agreement with the calculated value for Rh^{2+} . The almost perfect agreement shown in Fig. 5 is probably fortuitous. In the above process, we have neglected the fact that a small fraction (4%) of the Rh sites are occupied by FeII atoms. If we assume the moment of FeII atoms is $2.5 \mu_B$, as will be shown in the next section, the true rhodium moment in $\text{Fe}_{0.52}\text{Rh}_{0.48}$ should be $0.94 \mu_B$, and the form factor should be slightly modified.

The aspherical moment distribution, particularly pronounced in Rh, was already apparent in the Fourier

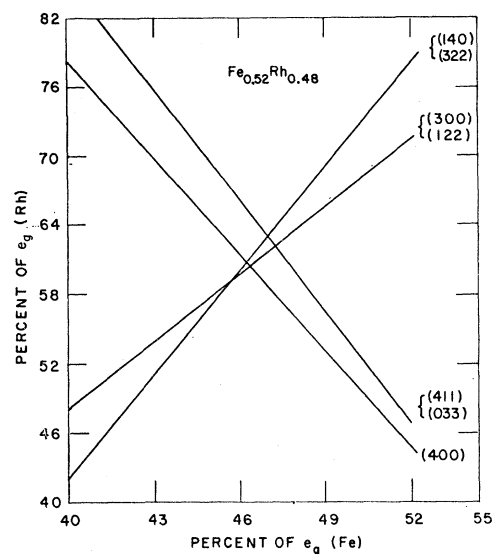


FIG. 6. Graphical determination of the fractions of e_g character for Fe and Rh in $\text{Fe}_{0.52}\text{Rh}_{0.48}$. 40% e_g corresponds to spherical symmetry.

densities shown in Figs. 3 and 4. A qualitative estimate was made by comparison of observed and calculated structure factors of three pairs of reflections, shown in Fig. 6, and (400) which shows the largest deviation from the spherical part. The form factor for e_g symmetry is given by

$$f(e_g) = \langle j_0 \rangle + \frac{3}{2} A \langle j_4 \rangle,$$

$$A = \frac{h^4 + k^4 + l^4 - 3(h^2k^2 + k^2l^2 + l^2h^2)}{(h^2 + k^2 + l^2)^2}.$$

The calculated values^{10,12} for $\langle j_4 \rangle$ are shown in the top part of Fig. 5. By a graphical method, the best solution for the percentage of e_g character in the spin density

¹² R. E. Watson and A. J. Freeman, Acta Cryst. 14, 27 (1961).

distribution was found to be $e_\theta(\text{Fe}) = 47 \pm 1\%$, $e_\theta(\text{Rh}) = 62 \pm 3\%$.

Spherical symmetry corresponds to 40% e_θ and 60% t_{2g} character.

IV. MOMENT DISTRIBUTION IN ALLOYS

Having established the values of the magnetic moments in the 48% Rh alloy, it is now of great interest to study the composition dependence of these moments, and in particular, that of FeII, namely Fe atoms on the Rh sites. These features were studied with polycrystalline samples of the 35 and 40% Rh alloys consisting of rectangular pillars $2 \times 5 \times 18$ mm. Both the polarized and unpolarized beam techniques were employed in these experiments. In the case of the former, a correction for depolarization of the neutron beam within the polycrystalline samples is

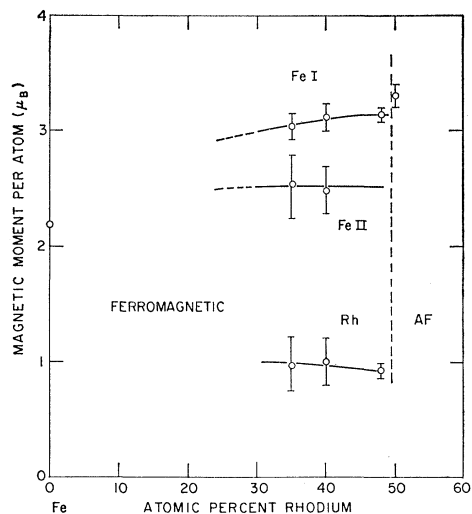


FIG. 7. Moment distributions in Fe-Rh alloys at room temperature.

required. With these in an applied field of 11 kOe, this correction turned out to be relatively small. The degree of chemical order in the 35% Rh sample was checked, and the order parameter was found to be at least 0.95.

The data were collected from a few reflections, (110), (200), (211), and (100). From these we can determine $F_M(+)=p_{\text{FeI}}+p_{\text{FeII}}+p_{\text{Rh}}$ and $F_M(-)=p_{\text{FeI}}-(p_{\text{FeII}}+p_{\text{Rh}})$. These, combined with the observed total moment by magnetic measurements, give the individual moments uniquely if we assume that the form factors of Fe and Rh determined for the 48% Rh alloy are unchanged in the other alloys.

The results are shown in Fig. 7. Large uncertainties, particularly in the moment of FeII, were introduced because of poor statistics in the powder diffraction data. It is quite clear, however, that μ_{FeII} is definitely smaller than μ_{FeI} despite its higher hyperfine field.

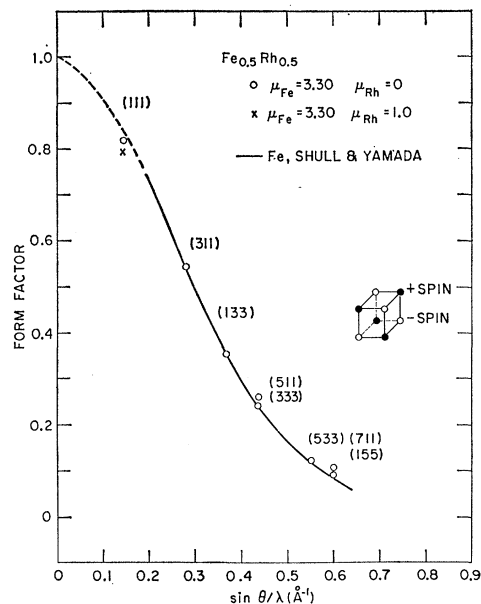


FIG. 8. Form factor of Fe in the antiferromagnetic phase of $\text{Fe}_{0.5}\text{Rh}_{0.5}$ at room temperature. The assumption that $\mu_{\text{Rh}} = 1.0 \mu_B$ does not introduce any noticeable change in the Fe form factors except for the (111) reflection.

V. ANTIFERROMAGNETIC PHASE IN $\text{Fe}_{0.5}\text{Rh}_{0.5}$

The basic magnetic structure of this phase was reported by Bertaut *et al.*⁵ and is shown as an insert to Fig. 8. This is the so-called *G*-type structure,¹³ in which every positive Fe spin is surrounded by six negative Fe spins. The magnetic unit cell edge is thus double that of the chemical cell. The Rh atom, which is located at the body-centered position, is now surrounded by four positive and four negative Fe spins. Thus the Rh moments may not be ordered. Even if they are ordered in the same *G*-type structure, the magnetic intensity is proportional to

$$F_M^2 = (\mu_{\text{Fe}} f_{\text{Fe}})^2 + (\mu_{\text{Rh}} f_{\text{Rh}})^2.$$

Since the angular dependence of f_{Fe} is quite different from that of f_{Rh} , it is possible in principle to solve for both μ_{Fe} and μ_{Rh} . In practice, however, F_M^2 is extremely insensitive to small changes of μ_{Rh} when $\mu_{\text{Rh}} f_{\text{Rh}} < 0.1 \mu_{\text{Fe}} f_{\text{Fe}}$.

The specimen consisted of a single crystal in the shape of a cylinder 1 mm in diameter and 5 mm in length with its axis along [110]. The magnetic peaks are indexed as hkl all odd by doubling the unit cell. Accurate intensity data were collected for both magnetic (h, k, l all odd) and nuclear peaks using an unpolarized beam. The absorption of the sample was relatively high ($\mu = 4.2 \text{ cm}^{-1}$) because of its large Rh content. A preliminary comparison of the observed structure factors with those calculated from the expressions

$$F_{\text{cal}} = (b_{\text{Fe}} \pm b_{\text{Rh}}) e^{-B(\sin \theta / \lambda)^2},$$

¹³ E. O. Wollan and W. C. Koehler, Phys. Rev. **100**, 545 (1955).

TABLE III. Nuclear structure factors of $\text{Fe}_{0.5}\text{Rh}_{0.5}$, in units of 10^{-12} cm. Statistical errors in F_{ob} are about 1%. Temperature factor $B=0.433 \text{ \AA}^2$ is included in F_{cal} .

hkl	F_{ob}	F_{cal}	hkl	F_{ob}	F_{cal}
011	1.47 ^a	1.50	100	0.356	0.362
200	1.46	1.46	111	0.358	0.354
211	1.43	1.43	300	0.332	0.329
022	1.39	1.40	122	0.326	0.329
222	1.32	1.33	311	0.324	0.321
400	1.28	1.26	322	0.293	0.298
033	1.25	1.24			
411	1.24	1.24			

^a Not included in the analysis because of a probable extinction effect.

in which⁹ $b_{\text{Fe}}=0.951 \times 10^{-12}$ cm and $b_{\text{Rh}}=0.60 \times 10^{-12}$ cm,¹⁴ revealed a systematic deviation opposite to what would have been expected in the case of imperfect chemical order. Therefore b_{Rh} was treated as a parameter to obtain better agreement. Assuming the chemical order is perfect, the new value of $b_{\text{Rh}}=0.585 \pm 0.005 \times 10^{-12}$ cm, together with a temperature factor $B=0.433 \text{ \AA}^2$, give the excellent agreement shown in Table III.

If chemical order is not complete, or the Rh content not 50%, it is clear that b_{Rh} would become even smaller. The above value of the temperature factor B was used to correct the observed magnetic structure factors. Magnetic intensities were also corrected for $\lambda/2$ contamination ($\sim 0.2\%$). Intensity data given in Table IV are average values of equivalent reflections. In view of the nuclear intensity agreement, it was assumed that no extinction correction was needed.

The magnetic reflections were first analyzed on the assumption that $\mu_{\text{Rh}}=0$. The Fe moment was determined from the (311) and (133) reflections using the form factor of metallic Fe. This gave

$$\mu_{\text{Fe}}=3.30 \mu_B.$$

The form factor f_{Fe} was then calculated for all the reflections using this moment value. There appears to be a slight systematic deviation of the observed form

TABLE IV. Magnetic structure factors F_M , in units of 10^{-12} cm, of antiferromagnetic $\text{Fe}_{0.5}\text{Rh}_{0.5}$ per chemical unit cell. Indices are based on the magnetic unit cell ($a=5.972 \text{ \AA}$). f_{Fe} is calculated on the assumption that $\mu_{\text{Fe}}=3.30 \mu_B$ and $\mu_{\text{Rh}}=0$.

hkl	$F_M(\pm 0.002)$	f_{Fe}
111	0.594	0.817
311	0.396	0.545
133	0.258	0.355
{333}	0.178	0.245
{511}	0.191	0.263
533	0.089	0.123
{155}	0.072	0.099
{711}	0.078	0.107

¹⁴ C. G. Shull and E. O. Wollan, *Solid State Physics*, edited by F. Seitz and D. Turnbull (Academic Press Inc., New York, 1956), Vol. 2, p. 137.

factor from the solid line representing that of metallic Fe as shown in Fig. 8. A part of this might be due to a systematic error introduced by an inaccurate temperature factor correction. (The polarized beam technique is free from this error since it is always the ratio, F_M/F_N , which is measured.)

Some estimate of the Rh moment can be made on the basis of the innermost magnetic peak. If we were to assume that the Rh moment remains $1.0 \mu_B$ in the antiferromagnetic state, then we obtain the value of the Fe form factor indicated by the cross in Fig. 8, which falls definitely below the extrapolated curve. Hence, our data does suggest that if the aligned moment on the Rh atoms in this magnetic state is not zero, it is at least lowered. However, the determination of the Fe moment is almost unaffected by this uncertainty in the Rh moment.

The asphericity of the Fe density distribution was estimated from two pairs of reflections, (511) and (333), and (711) and (155). The amount of e_g character is $48 \pm 3\%$, in good agreement with the value for FeI in the 48% Rh alloy.

VI. DISCUSSION

A. Magnetic Moments

Our results on the 48% and 50% alloys can now be compared with the moment values reported by Bertaut, de Bergevin, and Roult⁵ on the 53% alloy. Since the alloy compositions and temperature of measurements are different, only the ratio of the moments in the two magnetic phases are of any significance. They have reported $\mu_{\text{Fe}}=3.3 \mu_B$ in the antiferromagnetic phase at room temperature and $\mu_{\text{Fe}}=2.84 \mu_B$ and $\mu_{\text{Rh}}=0.80 \mu_B$ at 100°C , when the alloy is ferromagnetic. If allowance is made for the fact that the Mo^{3+} form factor¹⁵ was used in the derivation of the Rh moment, our present result are seen to be in good agreement with these values. The rhodium form factor determined in the present work drops off, as a function of scattering angle, somewhat more slowly than that of Mo^{3+} , as might be expected from their respective positions in the $4d$ series.

It is interesting to compare the magnetic moment of Fe in the antiferromagnetic phase with the Fe moment extrapolated from the ferromagnetic region. At room temperature, the extrapolated total moment is $3.88 \mu_B$ per unit cell (Fig. 1). Assuming that the ratio of μ_{Fe} to μ_{Rh} retains the value found in 48% Rh, we obtain a value of $3.0 \mu_B$ for the Fe moment. The observed moment is 10% higher than this value. This tendency may also be seen in Fig. 7, in which the moments were plotted as a function of composition.

At the transition from the ferromagnetic to the antiferromagnetic phase, the unit cell volume decreases³ by

¹⁵ M. K. Wilkinson, E. O. Wollan, H. R. Child, and J. W. Cable, *Phys. Rev.* **121**, 74 (1961).

1% and the hyperfine field at Fe⁵⁷ decreases by 6%.^{1,16} This is another illustration of the fact that, in this system, the hyperfine field is not related in any simple manner to the magnetic moments. We have already shown that FeII in the ferromagnetic phase has a smaller moment, despite its considerably higher hyperfine field, than FeI. We believe this is due to a different degree of polarization of the conduction electrons, with respect to which the hyperfine field is quite sensitive. At present there is, however, no direct experimental evidence to verify this assumption.

B. Form Factors

The form factors of Fe in the rhodium alloys are shown in Fig. 9, together with the previous results given for metallic Fe by Shull and Yamada⁹ and for Fe₃Al by Pickart and Nathans.⁸ The first striking characteristic is that the spherical parts of the form factors are very similar to each other, although the magnetic moments of the Fe atoms in their various surroundings are quite

TABLE V. Magnetic moments and their asphericities in several Fe alloys. 40% e_g character corresponds to spherical symmetry.

	Moment (μ_B)	e_g (%)
Fe Metal	2.18	0.53
Fe ₃ Al { FeI	2.18	0.60
{ FeII	1.50	0.48
Fe _{0.52} Rh _{0.48} FeI	3.14	0.47
Fe _{0.5} Rh _{0.5} FeI	3.30	0.48

different, as shown in Table V. However, the asphericity of the density distribution differs considerably.

Let us now compare the spherical part of the observed form factor with the calculated part. The most recent calculations available are the Hartree-Fock calculations with exact exchange polarization treatment by Freeman and Watson¹⁷ for the two configurations $3d^8$ and $3d^64s^2$. Somewhat surprisingly, the form factors for these two configurations turn out to be almost identical.¹⁸ This is in striking contrast to previous calculations by the same authors^{12,19} in which they obtained practically identical results for $3d^64s^2$ and $3d^6$ (Fe²⁺), but considerably lower values for $3d^8$.

Shull and Yamada compared their observed form

¹⁶ F. E. Obenshain, L. D. Roberts, and H. H. F. Wegener, Bull. Am. Phys. Soc. 8, 43 (1963).

¹⁷ A. J. Freeman and R. E. Watson (unpublished), quoted by Shull and Yamada (Ref. 9).

¹⁸ If the "true" calculated values of $3d^64s^2$ and $3d^8$ are really so close to each other, we cannot hope to distinguish the $3d$ configuration from the observed form factors.

¹⁹ A. J. Freeman and R. E. Watson, Acta Cryst. 14, 231 (1961).

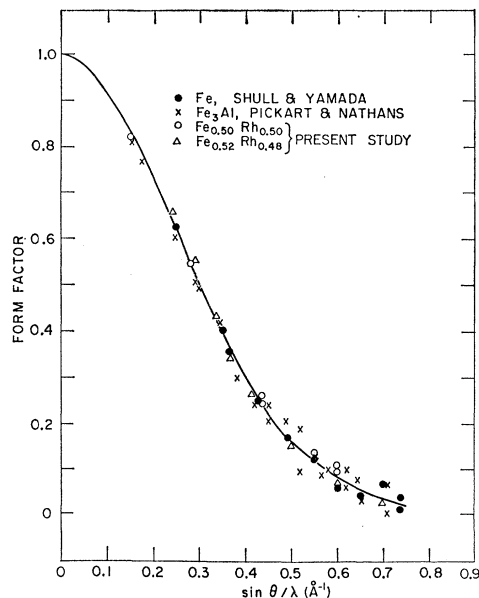


FIG. 9. Iron form factors determined for various alloys.

factors of Fe to the latest spin-polarized calculations and obtained a constant "ratio" between the two, namely, that the observed values were 10% higher than the calculated values. They attributed the difference to the polarization of 4s electrons assuming the calculated form factors were correct. Our data for the FeRh alloys as well as the previous results for Fe₃Al deviate from this constant ratio relation at the low-angle reflections with $\sin\theta/\lambda < 0.2 \text{ \AA}^{-1}$. If we include these points for comparison, better over-all agreement is obtained with the earlier calculations of Weiss and Freeman.²⁰ We believe that, at present, the proper procedure for obtaining information about the conduction electron polarization is to depend only on the experimental intensity observations and their Fourier transform. Our present data for the Fe-Rh alloys are not sufficient to draw significant conclusions concerning this point.

ACKNOWLEDGMENTS

We are very grateful to C. G. Shull, S. J. Pickart, D. E. Cox, and M. Blume for many stimulating discussions, to R. E. Watson and A. J. Freeman for providing us with their unpublished form factors, and to J. A. Ibers and W. C. Hamilton for the use of their three-dimensional Fourier program.

²⁰ R. J. Weiss and A. J. Freeman, Phys. Chem. Solids 10, 147 (1959).